2013 IEEE 10th International Symposium on Biomedical Imaging:
From Nano to Macro
San Francisco, CA, USA, April 7-11, 2013

PARALLEL PROXIMAL ALGORITHM FOR INTERIOR TOMOGRAPHY PROBLEMS IN X-RAY CT WITH TINY *A PRIORI* KNOWLEDGE

Minji Lee and Jong Chul Ye

Department of Bio & Brain Engineering,
Korea Advanced Institute of Science & Technology,
291 Daehak-ro, Yuseong-gu, Daejeon 305-701, Korea

ABSTRACT

Recently, it has been shown that interior tomography problems in x-ray CT can be uniquely determined if tiny subregions inside of the region of interest are known. The solution can be obtained by the projection onto convex sets (POCS) combined with the backprojection filtration algorithm. However, it is well-known that the convergence speed of POCS is slow; hence, to overcome the limitation, this paper employs a parallel proximal algorithm (PPXA) to simultaneously consider multiple convex constraints rather than projecting on each of them sequentially as in POCS. Our simulation results show that the solution for the interior tomography problem can be accurately obtained using PPXA with a much smaller number of iterations than POCS.

Index Terms— Interior tomography problem, parallel proximal algorithm, projection onto convex sets, backprojection filtration

1. INTRODUCTION

With the increasing demands for low-dose computed tomography (CT) to reduce radiation exposure on human bodies, we often encounter interior tomography problems, where only incomplete data are available due to the limited detector size or reduced illumination. Theoretical analysis has been extensively performed to show that the problem can be equivalently formulated as incomplete data extrapolation problem using differentiated backprojection data [1, 2]. More specifically, after backprojecting the differentiated projection data on chord lines, a 2D or 3D tomography problem using fan-beam or cone-beam CT can be converted into a set of 1D problems, which makes the interior tomography problem much simpler extrapolation problem. Based on this formulation, general imaging geometries that allow perfect reconstruction have been identified [1]. For example, if the imaging field of view (FOV) includes a background with air, then *a priori* knowledge of regions with air determines unique reconstruction. Another important example is that even though there exists no air interface in the FOV, if tiny regions within the FOV and boundary of the object are known *a priori*, an unique and stable solution can be computed [2]. Asides from the theoretical results, the authors in [1, 2] noted that the constraints due to *a priori* knowledge are convex and proposed a projection onto convex sets (POCS) algorithm to obtain the solution by sequentially projecting on the constraint set. They demonstrated excellent reconstruction results using POCS. However, one of the main limitations is that the POCS method finds the optimized solution by sequentially projecting the current solution onto each convex set, so its convergence speed is slow.

To address this problem, we employ a parallel proximal algorithm (PPXA) that has been recently proposed to address multiple convex constraints using a proximal algorithm [3]. More specifically, PPXA calculates the multiple proximal projections and computes a weighted average using Douglas Rachford splitting algorithm [3]. As the interior tomography problem can be converted into a 1D optimization problem with multiple convex constraints, it is nicely fitted into PPXA framework. In particular, the convex constraints in the interior tomography problem are just a set of indicator functions, so the corresponding proximal mappings are very simple, which makes the computational complexity of PPXA minimal. This paper explains how to apply PPXA to the interior tomography with *a priori* knowledge, and show that PPXA converges faster than POCS method. Even though the current formulation is based on 2D formulation, extension to 3D is straightforward and will be reported later.

2. BACKGROUNDS

2.1. Backprojection Filtration

Let $\mu(\vec{r})$ with $\vec{r} = (r_1, r_2)$ be the 2D attenuation coefficient function to be reconstructed, and its line integrals be represented as

$$p(s, \phi) = \int_{-\infty}^{\infty} dt \mu(s\vec{u}(\phi) + t\vec{u}^{\perp}(\phi)) \qquad (1)$$

where $\vec{u}(\phi) = (\cos\phi, \sin\phi)$ and $\vec{u}^{\perp}(\phi) = (-\sin\phi, \cos\phi)$. In this equation, $s \in \mathbb{R}$ is the signed distance from the origin

This work was supported by the National Research Foundation of Korea (NRF) grant No. 20120000173 funded by the Korea government (MEST)

to the line, and $\phi \in [0, 2\pi)$ represents the angle of the line. Here, $p(s, \phi)$ is the projection. From this projection data, differentiated backprojection (DBP) can be computed as

$$b(\vec{r}) = -\frac{1}{2\pi} \int_{\phi_0}^{\phi_0+\pi} d\phi \left[\frac{\partial p(s, \phi)}{\partial s} \right]_{s=\vec{r}\cdot\vec{u}(\phi)} \quad (2)$$

with some fixed arbitrary angle ϕ_0. Now, the DBP $b(\vec{r})$ and the attenuation coefficient function $\mu(\vec{r})$ have the relationship as

$$b(\vec{r}) = \frac{1}{\pi} \text{P.V.} \int_{-\infty}^{\infty} \frac{dt}{t} \mu(\vec{r} - t\vec{n}) = (\mathcal{H}_{\mathcal{L}}\mu)(\vec{r}) \quad (3)$$

where $\vec{n} = (-\sin\phi_0, \cos\phi_0) = \vec{u}^{\perp}(\phi_0)$. Here, $\mathcal{H}_{\mathcal{L}}$ dentes the 1D Hilbert transform along $\mathcal{L}$, and P.V. denotes the Cauchy principal value. This relation can be considered as the 1D Hilbert transform of μ along the line $\mathcal{L}$ that is parallel to $\vec{n}$. Thus, we can restrict the original 2D object $\mu(\vec{r})$ and DBP $b(\vec{r})$ to the 1D functions $f(x)$ and $g(x)$ along the line $\mathcal{L}$, respectively; and if $f(x)$ is a continuous function with support on the interval $x \in [a_1, a_2]$, the relationship between $f(x)$ and $g(x)$ can be written as

$$g(x) = (\mathcal{H}f)(x) = \frac{1}{\pi} \text{P.V.} \int_{a_1}^{a_2} \frac{dx'}{x - x'} f(x'). \quad (4)$$

In this equation, $g(x)$ is available, and we do not know $f(x)$. So, the inversion of (4) is necessary for reconstruction. According to [2], by using the inversion formula for the truncated Hilbert transform, $f(x)$ can be recovered from $g(x)$:

$$f(x) = \frac{1}{\sqrt{(a_2 - x)(x - a_1)}} \left[\frac{1}{\pi} \text{P.V.} \int_{a_1}^{a_2} \frac{dx'}{x' - x} \times g(x') \sqrt{(a_2 - x')(x' - a_1)} + C_f \right] \quad (5)$$

where $C_f = \frac{1}{\pi} \int_{a_1}^{a_2} dx f(x)$ which can be obtained from the projection data. For the exact reconstruction, the sufficient conditions need to be satisfied, implying that the $\mathcal{L}$ should have no truncation, and the line integrals $p(s, \phi)$ should be known for $\phi \in [\phi_0, \phi_0 + \pi]$. If the sufficient conditions are not satisfied, the analytic reconstruction is not available, which is known as interior problem [2].

2.2. Interior Tomography with *a priori* Knowledge

Among various types of interior tomography problems, this paper considers the case in [2], where tiny regions of interior FOV are known. Extension of the proposed method for other interior tomography problems is straightforward and will be reported later. More specifically, as in Fig.1, the support of $f(x)$ is $[a_1, a_2]$, which is assumed to be known, and the projection data are available only for $[b_1, b_2]$. It means we know

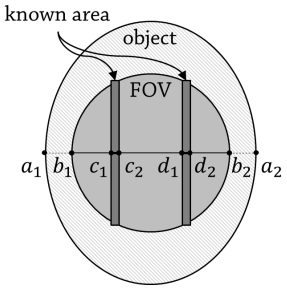

Fig. 1. Interior problem with tiny *a priori* knowledge [2].

$g(x)$ correctly only for $[b_1, b_2]$, so $f(x)$ cannot be recovered by (5). However, if we have some known regions in $[b_1, b_2]$ such as $[c_1, c_2]$ and $[d_1, d_2]$, the theory says that $f(x)$ can be determined uniquely [2]. In [2], using *a priori* knowledge, the five convex constraints for $\tilde{f}(x) \in L^2(\mathbb{R})$ were identified:

$C_1 = \{\tilde{f}(x) \in L^2(\mathbb{R}) : (\mathcal{H}\tilde{f})(x) = g(x), x \in [b_1, b_2]\}$
$C_2 = \{\tilde{f}(x) \in L^2(\mathbb{R}) : \tilde{f}(x) = f(x), x \in [c_1, c_2] \cup [d_1, d_2]\}$
$C_3 = \{\tilde{f}(x) \in L^2(\mathbb{R}) : \tilde{f}(x) = 0, x \notin [a_1, a_2]\}$
$C_4 = \{\tilde{f}(x) \in L^2(\mathbb{R}) : \tilde{f}(x) \geq 0, x \in [a_1, a_2]\}$
$C_5 = \{\tilde{f}(x) \in L^2(\mathbb{R}) : \frac{1}{\pi} \int_{a_1}^{a_2} dx \tilde{f}(x) = C_f\}$,

and the optimized solution of $\tilde{f}(x)$ was solved by POCS.

More specifically, if P_{C_j} is the orthogonal projector onto the convex set C_j for $j = 1, \ldots, 5$, the iteration of the POCS algorithm can be described as

$$f_k(x) = P_{C_5} P_{C_4} P_{C_3} P_{C_2} P_{C_1} f_{k-1}(x) \quad (6)$$

with some arbitrary initialization $f_0(x)$. This algorithm converges to one element of the intersection of the constraints if the intersection is not empty. However, it is well-known that POCS has slow convergence, so we are interested in developing a new algorithm.

3. PROPOSED METHOD

In this section, we show that the interior tomography problem can be addressed using a parallel proximal algorithm.

3.1. Proximity Operator

If $\Gamma_0(\mathbb{R}^N)$ is the class of lower semicontinuous convex functions from $\mathbb{R}^N$ to $(-\infty, +\infty]$, the proximity operator of $\varphi \in \Gamma_0(\mathbb{R}^N)$ is defined as

$$\text{prox}_{\varphi} : \mathbb{R}^N \to \mathbb{R}^N : u \mapsto \arg\min_{v \in \mathbb{R}^N} \frac{1}{2}\|v - u\|^2 + \varphi(v), \quad (7)$$

The proximal mapping has been extensively used to derive new class of convex optimization algorithms [3]. However, in most cases, the number of convex penalty terms are limited to one. In our interior tomography problems, there exist multiple convex constraints, so we need a new algorithm that fit into the interior tomography problem [3].

3.2. Parallel Proximal Algorithm

PPXA is a new class of proximal mapping algorithms that address multiple convex constraints [4]

$$\text{Find } \hat{\xi} = \arg\min_{\xi\in\mathbb{R}^N} \sum_{j=1}^{J} \varphi_j(\xi) \tag{8}$$

where $\varphi_j \in \Gamma_0(\mathbb{R}^N)$ and $J \geq 3$. Algorithm 1 describes a PPXA implementation.

Algorithm 1 Parallel proximal algorithm (PPXA)

1: Set $\gamma \in (0, +\infty)$.
2: Set $(\omega_j)_{1\leq j\leq J} \in (0,1]^J$ satisfying $\sum_{j=1}^{J} \omega_j = 1$.
3: Set $(u_{j,0})_{1\leq j\leq J} \in (\mathbb{R}^N)^J$.
4: Set $\xi_0 = \sum_{j=1}^{J} \omega_j u_{j,0}$.
5: **for** $k = 0, 1, \ldots$ **do**
6: **for** $j = 1, \ldots, J$ **do**
7: $p_{j,k} = \text{prox}_{\gamma\varphi_j/\omega_j} u_{j,k} + a_{j,k}$
8: **end for**
9: $p_k = \sum_{j=1}^{J} \omega_j p_{j,k}$
10: Set $\lambda_k \in (0, 2)$
11: **for** $j = 1, \ldots, J$ **do**
12: $u_{j,k+1} = u_{j,k} + \lambda_k(2p_k - \xi_k - p_{j,k})$
13: **end for**
14: $\xi_{k+1} = \xi_k + \lambda_k(p_k - \xi_k)$
15: **end for**

PPXA needs real constants γ and $(\omega_j)_{1\leq j\leq J}$, and ω_j is the weight for the proximity operator of φ_j. The relaxation parameter λ_k can be chosen differently at each step, and the data fidelity term $a_{j,k}$ is included when calculating a proximal vector $p_{j,k}$ in line 7. The main feature of this algorithm is that at each iteration k, the proximal vectors $(p_{j,k})_{1\leq j\leq J}$ and the auxiliary vectors $(u_{j,k})_{1\leq j\leq J}$ can be computed simultaneously. This is the main difference from POCS method, and it makes the convergence of PPXA faster.

In our interior tomography problem, all the constraints can be formulated using a set of indicator functions. More specifically, the indicator function of convex C is

$$\iota_C(x) = \begin{cases} 0, & \text{if } x \in C \\ +\infty, & \text{if } x \notin C \end{cases}, \tag{9}$$

and its proximity operator is the projection onto C, P_C [3]. With this definition, we can make indicator functions for each constraint C_1-C_4 as

$$\iota_{C_1}(\tilde{f}(x)) = \begin{cases} 0, & \text{if } (\mathcal{H}\tilde{f})(x) = g(x), x \in [b_1, b_2] \\ +\infty, & \text{otherwise} \end{cases}$$

$$\iota_{C_2}(\tilde{f}(x)) = \begin{cases} 0, & \text{if } \tilde{f}(x) = f(x), x \in [c_1, c_2] \cup [d_1, d_2] \\ +\infty, & \text{otherwise} \end{cases}$$

$$\iota_{C_3}(\tilde{f}(x)) = \begin{cases} 0, & \text{if } \tilde{f}(x) = 0, x \notin [a_1, a_2] \\ +\infty, & \text{otherwise} \end{cases}$$

$$\iota_{C_4}(\tilde{f}(x)) = \begin{cases} 0, & \text{if } \tilde{f}(x) \geq 0, x \in [a_1, a_2] \\ +\infty, & \text{otherwise} \end{cases}$$

and for C_5, even though we do not make a indicator function, this constraint can be easily incorporated as constant C_f in computing the truncated Hilbert transform (5). Now, the minimization problem for the interior tomography with *a priori* knowledge can be formulated as

$$\text{Find } \hat{f}(x) = \arg\min_{\tilde{f}(x)\in L^2(\mathbb{R})} \sum_{j=1}^{4} \iota_{C_j}(\tilde{f}(x)), \tag{10}$$

and PPXA can be applied to solve (10). As we know, the proximity operator of the indicator function of C is the projection onto C, so in Algorithm 1, $\text{prox}_{\gamma\varphi_j/\omega_j}$ will be replaced with P_{C_j}. Note that this algorithm can be converged under the following assumptions [4], which are trivially satisfied in our interior tomography problem.

1) $\lim_{\|\xi\|\to+\infty} \varphi_1(\xi) + \cdots + \varphi_J(\xi) = +\infty$.
2) $\cap_{j=1}^{J} \text{rint dom } \varphi_j \neq \varnothing$.
3) $(\forall j \in \{1, \ldots, J\}) \sum_{k\in\mathbb{N}} \lambda_k \|a_{j,k}\| < +\infty$.
4) $\sum_{k\in\mathbb{N}} \lambda_k(2 - \lambda_k) = +\infty$.

4. SIMULATION RESULTS

A simulation geometry for the interior problem of computed tomography with *a priori* knowledge is described in Fig. 1. The FOV is completely inside the object, and we have small known regions in FOV. By decomposing the 2D image into the 1D horizontal lines after applying DBP, we can cover all FOV with lines intersecting the two known regions except the small top and bottom areas, and a set of 1D problems corresponding to each line is reconstructed using PPXA. For simulation, we use 2D Shepp-Logan phantom, and the size of the object is 256^2 pixels with 0.5^2mm^2 size of the pixel. The 800 views of projections are sampled for 360°.

The reconstruction results of POCS and PPXA after 100 iterations are shown in Fig. 2. The reconstruction images of both algorithms look similar, but in the line profile, the result of PPXA is more accurate. In the line profile of the POCS result, we can see the small known regions where the intensity values are accurate. Besides those regions, the intensities of the object still have differences from the ground truth. However, the line profile of the PPXA result is almost similar to the original phantom.

Fig. 3 shows the difference images between reconstruction and the ground truth. All images are displayed in same display scale, and the intensity value same as the background represents no error. In POCS results, the two gray lines are apparent, which means the other areas are not accurate. The error after 200 iterations decreases, but is still significant. In contrast, in PPXA case, the error only after 100 iterations does not have distinguishable known areas because the areas

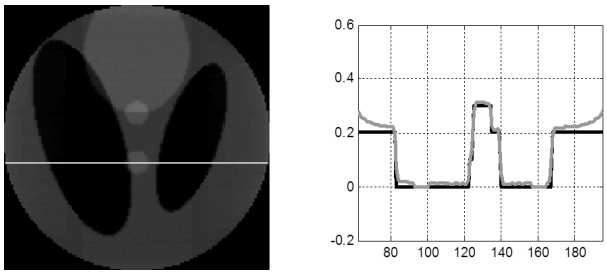

(a) POCS_{100} (b) POCS_{100}

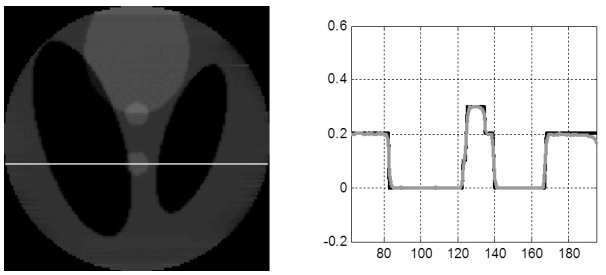

(c) PPXA_{100} (d) PPXA_{100}

Fig. 2. Reconstruction images and line profiles after 100 iterations.

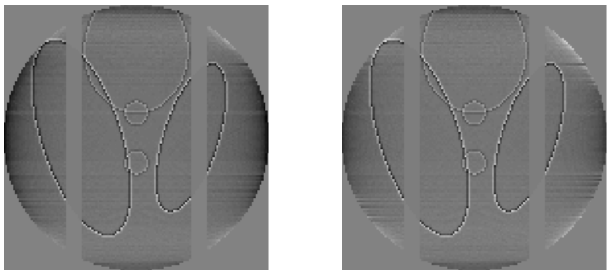

(a) POCS_{100} (b) POCS_{200}

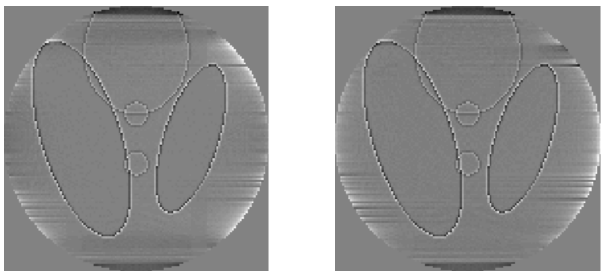

(c) PPXA_{100} (d) PPXA_{200}

Fig. 3. Error images after 100 or 200 iterations.

near the known regions are very accurate, and the overall error after 100 iterations is much less than the error of POCS after 200 iterations. The convergence in term of mean square error (MSE) is shown in Fig. 4. POCS method has overshoot point at the iteration number about 20, and PPXA has two big overshoots before about 50 iterations. Note that MSE value is not necessary to decrease monotonically since this is not what we minimize. We cannot plot the cost functions either since the cost functions are sum of indicator functions that have infinite values until convergence. Therefore, the overshoots in MSE domain are normally expected. Even though there exist overshoots of MSE values during the initial few iterations, after the overshoots, both algorithms converge, but PPXA converges much faster than POCS. Using PPXA, after only 80 iterations, convergence has been achieved.

5. CONCLUSIONS

Using differentiated backprojection and Hilbert transform, interior tomography problem can be converted to a set of 1D inverse problems. In particular, the interior tomography problem with tiny known areas and support of the object can be converted into an optimization problem with multiple convex constraints. Even though originally proposed POCS method for this problem provided excellent reconstruction, the convergence rate was shown slow. Hence, in this paper, we employed PPXA algorithm to overcome the limitation of POCS. Using numerical experiments, we demonstrated that PPXA provides much faster convergence and improves reconstruction result in the local tomography problem compared to POCS method.

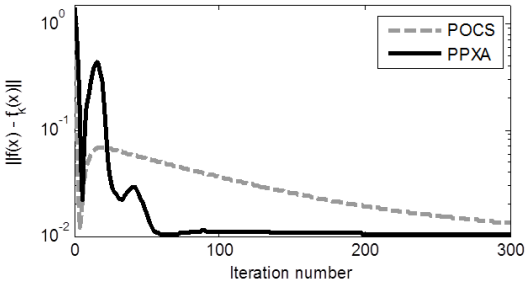

Fig. 4. MSE convergence of POCS and PPXA.

6. REFERENCES

[1] M. Defrise, F. Noo, R. Clackdoyle, and H. Kudo, "Truncated Hilbert transform and image reconstruction from limited tomographic data," *Inverse Problems*, vol. 22, no. 3, pp. 1037, 2006.

[2] M. Courdurier, F. Noo, M. Defrise, and H. Kudo, "Solving the interior problem of computed tomography using *a priori* knowledge," *Inverse problems*, vol. 24, no. 6, pp. 065001, 2008.

[3] P.L. Combettes and J.C. Pesquet, "Proximal splitting methods in signal processing," *Fixed-Point Algorithms for Inverse Problems in Science and Engineering*, pp. 185–212, 2011.

[4] N. Pustelnik, C. Chaux, and J. Pesquet, "Parallel proximal algorithm for image restoration using hybrid regularization," *IEEE Transactions on Image Processing*, vol. 20, no. 9, pp. 2450–2462, 2011.